

# Thermal axion production in the primordial quark-gluon plasma

Peter Graf and Frank Daniel Steffen

Max-Planck-Institut für Physik, Föhringer Ring 6, D-80805 Munich, Germany

We calculate the rate for thermal production of axions via scattering of quarks and gluons in the primordial quark-gluon plasma. To obtain a finite result in a gauge-invariant way that is consistent to leading order in the strong gauge coupling, we use systematic field theoretical methods such as hard thermal loop resummation and the Braaten–Yuan prescription. The thermally produced yield, the decoupling temperature, and the density parameter are computed for axions with a mass below 10 meV. In this regime, with a Peccei–Quinn scale above  $6 \times 10^8$  GeV, the associated axion population can still be relativistic today and can coexist with the axion cold dark matter condensate.

PACS numbers: 14.80.Va, 98.80.Cq, 95.35.+d, 95.30.Cq

*Introduction*—If the Peccei–Quinn (PQ) mechanism is the explanation of the strong CP problem, axions will pervade the Universe as an extremely weakly interacting light particle species. In fact, an axion condensate is still one of the most compelling explanations of the cold dark matter in our Universe [1, 2]. While such a condensate would form at temperatures  $T \lesssim 1$  GeV, additional populations of axions can originate from processes at much higher temperatures. Even if the reheating temperature  $T_R$  after inflation is such that axions were never in thermal equilibrium with the primordial plasma, they can be produced efficiently via scattering of quarks and gluons. Here we calculate for the first time the associated thermal production rate consistent to leading order in the strong gauge coupling  $g_s$  in a gauge-invariant way. The result allows us to compute the associated relic abundance and to estimate the critical  $T_R$  value below which our considerations are relevant. For a higher value of  $T_R$ , one will face the case in which axions were in thermal equilibrium with the primordial plasma before decoupling at the temperature  $T_D$  as a hot thermal relic [1, 3]. The obtained critical  $T_R$  value can then be identified with the axion decoupling temperature  $T_D$ .

We focus on the model-independent axion ( $a$ ) interactions with gluons given by the Lagrangian<sup>1</sup>

$$\mathcal{L}_a = \frac{g_s^2}{32\pi^2 f_{\text{PQ}}} a G_{\mu\nu}^b \tilde{G}^{b\mu\nu}, \quad (1)$$

with the gluon field strength tensor  $G_{\mu\nu}^b$ , its dual  $\tilde{G}^{b\mu\nu} = \epsilon_{\mu\nu\rho\sigma} G^{b\rho\sigma}/2$ , and the scale  $f_{\text{PQ}}$  at which the PQ symmetry is broken spontaneously. Numerous laboratory, astrophysical, and cosmological studies point to

$$f_{\text{PQ}} \gtrsim 6 \times 10^8 \text{ GeV}, \quad (2)$$

which implies that axions are stable on cosmological timescales [4, 5]. Considering this  $f_{\text{PQ}}$  range, we can

neglect axion production via  $\pi\pi \rightarrow \pi a$  in the primordial hot hadronic gas [6, 7]. Moreover, Primakoff processes such as  $e^- \gamma \rightarrow e^- a$  are not taken into account since they depend on the axion model and are usually far less efficient in the early Universe [8].

We assume a standard thermal history and refer to  $T_R$  as the initial temperature of the radiation-dominated epoch. While inflation models can point to  $T_R$  well above  $10^{10}$  GeV, we focus on the case  $T_R < f_{\text{PQ}}$  such that no PQ symmetry restoration takes place after inflation.

Related studies exist. The decoupling of axions out of thermal equilibrium with the primordial quark-gluon plasma (QGP) was considered in Refs. [1, 3]. While the same QCD processes are relevant, our study treats the thermal production of axions that were never in thermal equilibrium. Moreover, we use hard thermal loop (HTL) resummation [9] and the Braaten–Yuan prescription [10] which allow for a systematic gauge-invariant treatment of screening effects in the QGP. In fact, that prescription was introduced on the example of axion production in a hot QED plasma [10]; see also Ref. [11].

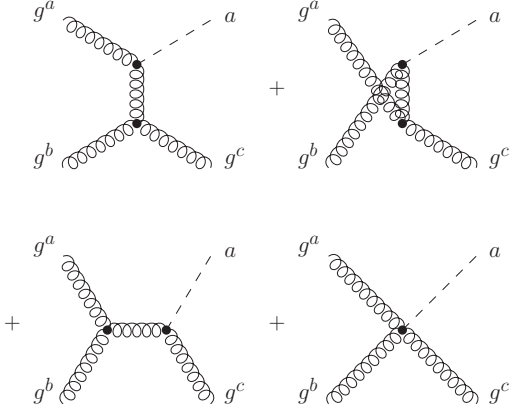
*Thermal production rate*—Let us calculate the thermal production rate of axions with energies  $E \gtrsim T$  in the hot QGP. The relevant  $2 \rightarrow 2$  scattering processes involving (1) are shown in Fig. 1. The corresponding squared matrix elements are listed in Table I, where  $s = (P_1 + P_2)^2$  and  $t = (P_1 - P_3)^2$  with  $P_1, P_2, P_3$ , and  $P$  referring to

TABLE I. Squared matrix elements for axion ( $a$ ) production in 2-body processes involving quarks of a single chirality ( $q_i$ ) and gluons ( $g^a$ ) in the high-temperature limit,  $T \gg m_i$ , with the  $SU(N_c)$  color matrices  $f^{abc}$  and  $T_{ji}^a$ . Sums over initial and final state spins have been performed.

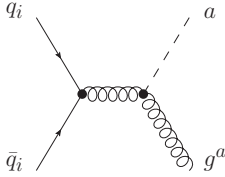
Label $i$	Process $i$	$ M_i ^2 / \left( \frac{g_s^6}{128\pi^4 f_{\text{PQ}}^2} \right)$
A	$g^a + g^b \rightarrow g^c + a$	$-4 \frac{(s^2 + st + t^2)^2}{st(s+t)}  f^{abc} ^2$
B	$q_i + \bar{q}_j \rightarrow g^a + a$	$\left( \frac{2t^2}{s} + 2t + s \right)  T_{ji}^a ^2$
C	$q_i + g^a \rightarrow q_j + a$	$\left( -\frac{2s^2}{t} - 2s - t \right)  T_{ji}^a ^2$

<sup>1</sup> The relation of  $f_{\text{PQ}}$  to the VEV  $\langle \phi \rangle$  that breaks the  $U(1)_{\text{PQ}}$  symmetry depends on the axion model and the associated domain wall number  $N$ :  $f_{\text{PQ}} \propto \langle \phi \rangle / N$ ; cf. [1, 2] and references therein.

**Process A:**  $g^a + g^b \rightarrow g^c + a$



**Process B:**  $q_i + \bar{q}_j \rightarrow g^a + a$



**Process C:**  $q_i + g^a \rightarrow q_j + a$  (crossing of B)

FIG. 1. The  $2 \rightarrow 2$  processes for axion production in the QGP. Process C exists also with antiquarks  $\bar{q}_{i,j}$  replacing  $q_{i,j}$ .

the particles in the given order. Working in the limit,  $T \gg m_i$ , the masses of all particles involved have been neglected. Sums over initial and final spins have been performed. For quarks, the contribution of a single chirality is given. The results obtained for processes A and C point to potential infrared (IR) divergences associated with the exchange of soft (massless) gluons in the  $t$ -channel and  $u$ -channel. Here screening effects of the plasma become relevant. To account for such effects, the QCD Debye mass  $m_D = \sqrt{3}m_g$  with  $m_g = g_s T \sqrt{N_c + (n_f/2)}/3$  for  $N_c = 3$  colors and  $n_f = 6$  flavors was used in Ref. [3]. In contrast, our calculation relies on HTL resummation [9, 10] which treats screening effects more systematically.

Following Ref. [10], we introduce a momentum scale  $k_{\text{cut}}$  such that  $g_s T \ll k_{\text{cut}} \ll T$  in the weak coupling limit  $g_s \ll 1$ . This separates soft gluons with momentum transfer of order  $g_s T$  from hard gluons with momentum transfer of order  $T$ . By summing the respective soft and hard contributions, the finite rate for thermal production of axions with  $E \gtrsim T$  is obtained in leading order in  $g_s$ ,

$$E \frac{dW_a}{d^3p} = E \frac{dW_a}{d^3p} \Big|_{\text{soft}} + E \frac{dW_a}{d^3p} \Big|_{\text{hard}}, \quad (3)$$

which is independent of  $k_{\text{cut}}$ ; cf. (5) and (7) given below.

In the region with  $k < k_{\text{cut}}$ , we obtain the soft contribution from the imaginary part of the thermal axion

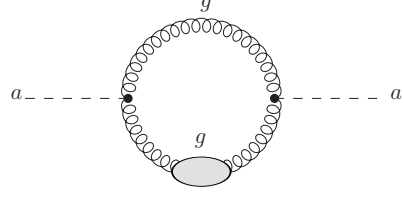


FIG. 2. Leading contribution to the axion self-energy for soft gluon momentum transfer and hard axion energy. The blob on the gluon line denotes the HTL-resummed gluon propagator.

self-energy with the ultraviolet cutoff  $k_{\text{cut}}$ ,

$$E \frac{dW_a}{d^3p} \Big|_{\text{soft}} = -\frac{f_B(E)}{(2\pi)^3} \text{Im} \Pi_a(E + i\epsilon, \vec{p}) \Big|_{k < k_{\text{cut}}} \quad (4)$$

$$= E f_B(E) \frac{3m_g^2 g_s^4 (N_c^2 - 1) T}{8192\pi^8 f_{\text{PQ}}^2} \left[ \ln\left(\frac{k_{\text{cut}}^2}{m_g^2}\right) - 1.379 \right] \quad (5)$$

with the equilibrium phase space density for bosons (fermions)  $f_{\text{B(F)}}(E) = [\exp(E/T) \mp 1]^{-1}$ . Our derivation of (5) follows Ref. [10]. The leading order contribution to  $\text{Im} \Pi_a$  for  $k < k_{\text{cut}}$  and  $E \gtrsim T$  comes from the Feynman diagram shown in Fig. 2. Because of  $E \gtrsim T$ , only one of the two gluons can have a soft momentum. Thus only one effective HTL-resummed gluon propagator is needed.

In the region with  $k > k_{\text{cut}}$ , bare gluon propagators can be used since  $k_{\text{cut}}$  provides an IR cutoff. From the results given in Table I weighted with appropriate multiplicities, statistical factors, and phase space densities, we then obtain the (angle-averaged) hard contribution

$$\begin{aligned} E \frac{dW_a}{d^3p} \Big|_{\text{hard}} &= \frac{1}{2(2\pi)^3} \int \frac{d\Omega_p}{4\pi} \int \left[ \prod_{j=1}^3 \frac{d^3 p_j}{(2\pi)^3 2E_j} \right] \\ &\times (2\pi)^4 \delta^4(P_1 + P_2 - P_3 - P) \Theta(k - k_{\text{cut}}) \\ &\times \sum f_1(E_1) f_2(E_2) [1 \pm f_3(E_3)] |M_{1+2 \rightarrow 3+a}|^2 \\ &= E \frac{g_s^6 (N_c^2 - 1)}{512\pi^7 f_{\text{PQ}}^2} \left\{ n_f \frac{f_B(E) T^3}{48\pi} \ln(2) \right. \\ &+ \left( N_c + \frac{n_f}{2} \right) \frac{f_B(E) T^3}{48\pi} \left[ \ln\left(\frac{T^2}{k_{\text{cut}}^2}\right) + \frac{17}{3} - 2\gamma + \frac{2\zeta'(2)}{\zeta(2)} \right] \\ &\left. + N_c (I_{\text{BBB}}^{(1)} - I_{\text{BBB}}^{(3)}) + n_f (I_{\text{FBF}}^{(1)} + I_{\text{FBF}}^{(3)}) \right\} \quad (7) \end{aligned}$$

with Euler's constant  $\gamma$ , Riemann's zeta function  $\zeta(z)$ ,

$$\begin{aligned} I_{\text{BBB}}^{(1)} &= \frac{1}{32\pi^3} \int_0^\infty dE_3 \int_0^{E+E_3} dE_1 \ln\left(\frac{|E_1 - E_3|}{E_3}\right) \\ &\times \left\{ -\Theta(E_1 - E_3) \frac{d}{dE_1} \left[ f_{\text{BBB(FBF)}} \frac{E_2^2}{E^2} (E_1^2 + E_3^2) \right] \right. \\ &+ \Theta(E_3 - E_1) \frac{d}{dE_1} [f_{\text{BBB(FBF)}} (E_1^2 + E_3^2)] \\ &\left. + \Theta(E - E_1) \frac{d}{dE_1} \left[ f_{\text{BBB(FBF)}} \left( \frac{E_1^2 E_2^2}{E^2} - E_3^2 \right) \right] \right\}, \quad (8) \end{aligned}$$

$$\begin{aligned}
I_{\text{BBB(FFB)}}^{(3)} &= \frac{1}{32\pi^3} \int_0^\infty dE_3 \int_0^{E+E_3} dE_2 f_{\text{BBB(FFB)}} \\
&\times \left\{ \Theta(E-E_3) \frac{E_1^2 E_3^2}{E^2(E_3+E)} + \Theta(E_3-E) \frac{E_2^2}{E_3+E} \right. \\
&\quad \left. + [\Theta(E_3-E)\Theta(E_2-E_3) - \Theta(E-E_3)\Theta(E_3-E_2)] \right. \\
&\quad \left. \times \frac{E_2-E_3}{E^2} [E_2(E_3-E) - E_3(E_3+E)] \right\}, \quad (9)
\end{aligned}$$

$$f_{\text{BBB,FBF,FFB}} = f_1(E_1)f_2(E_2)[1 \pm f_3(E_3)]. \quad (10)$$

The sum in (6) is over all axion production processes  $1+2 \rightarrow 3+a$  viable with (1). The colored particles 1–3 were in thermal equilibrium at the relevant times. Performing the calculation in the rest frame of the plasma,  $f_i$  are thus described by  $f_{\text{F/B}}$  depending on the respective spins. Shorthand notation (10) indicates the corresponding combinations, where  $+$  ( $-$ ) accounts for Bose enhancement (Pauli blocking) when particle 3 is a boson (fermion). With any initial axion population diluted away by inflation and  $T$  well below  $T_{\text{D}}$  so that axions are not in thermal equilibrium, the axion phase space density  $f_a$  is negligible in comparison to  $f_{\text{F/B}}$ . Thereby, axion disappearance reactions ( $\propto f_a$ ) are neglected as well as the respective Bose enhancement ( $1+f_a \approx 1$ ). Details on the methods applied to obtain our results (7), (8), and (9) can be found in Ref. [11].

*Relic axion abundance*—We now calculate the thermally produced (TP) axion yield  $Y_a^{\text{TP}} = n_a/s$ , where  $n_a$  is the corresponding axion number density and  $s$  the entropy density. For  $T$  sufficiently below  $T_{\text{D}}$ , the evolution of the thermally produced  $n_a$  with cosmic time  $t$  is governed by the Boltzmann equation

$$\frac{dn_a}{dt} + 3Hn_a = \int d^3p \frac{dW_a}{d^3p} = W_a. \quad (11)$$

Here  $H$  is the Hubble expansion rate, and the collision term is the integrated thermal production rate

$$W_a = \frac{\zeta(3)g_s^6 T^6}{64\pi^7 f_{\text{PQ}}^2} \left[ \ln \left( \frac{T^2}{m_g^2} \right) + 0.406 \right]. \quad (12)$$

Assuming conservation of entropy per comoving volume element, (11) can be written as  $dY_a^{\text{TP}}/dt = W_a/s$ . Since thermal axion production proceeds basically during the hot radiation dominated epoch, i.e., well above the temperature of radiation-matter equality  $T_{\text{mat=rad}}$ , one can change variables from cosmic time  $t$  to temperature  $T$  accordingly. With initial temperature  $T_{\text{R}}$  at which  $Y_a^{\text{TP}}(T_{\text{R}}) = 0$ , the relic axion yield today is given by

$$\begin{aligned}
Y_a^{\text{TP}} &\approx Y_a^{\text{TP}}(T_{\text{mat=rad}}) = \int_{T_{\text{mat=rad}}}^{T_{\text{R}}} dT \frac{W_a(T)}{Ts(T)H(T)} \\
&= 18.6g_s^6 \ln \left( \frac{1.501}{g_s} \right) \left( \frac{10^{10} \text{ GeV}}{f_{\text{PQ}}} \right)^2 \left( \frac{T_{\text{R}}}{10^{10} \text{ GeV}} \right). \quad (13)
\end{aligned}$$

This result is shown by the diagonal lines in Fig. 3 for cosmological scenarios with different  $T_{\text{R}}$  values ranging from

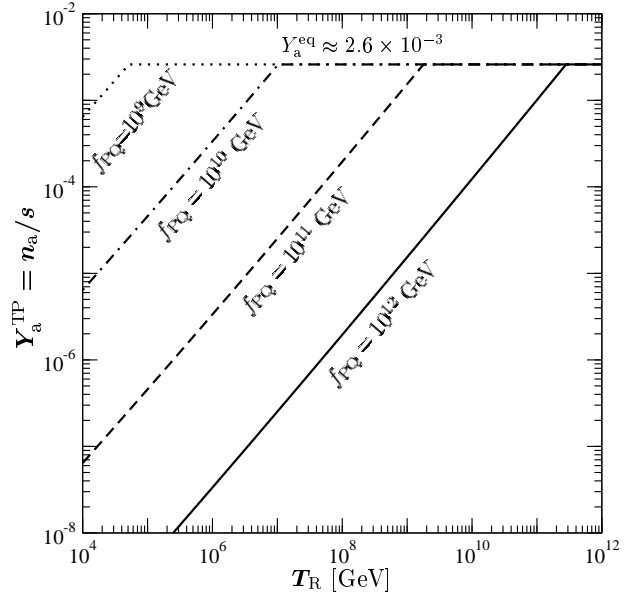


FIG. 3. The relic axion yield today originating from thermal processes in the primordial plasma for cosmological scenarios characterized by different  $T_{\text{R}}$  values covering the range from  $10^4$  to  $10^{12}$  GeV. The dotted, dash-dotted, dashed, and solid lines are obtained for  $f_{\text{PQ}} = 10^9, 10^{10}, 10^{11},$  and  $10^{12}$  GeV.

$10^4$  to  $10^{12}$  GeV. Here we use  $g_s = g_s(T_{\text{R}})$  as described by the 1-loop renormalization group evolution [5]

$$g_s(T_{\text{R}}) = \left[ g_s^{-2}(M_Z) + \frac{11N_c - 2n_f}{24\pi^2} \ln \left( \frac{T_{\text{R}}}{M_Z} \right) \right]^{-1/2} \quad (14)$$

where  $g_s^2(M_Z)/(4\pi) = 0.1172$  at  $M_Z = 91.188$  GeV. Note that (13) is only valid when axion disappearance processes can be neglected. In scenarios in which  $T_{\text{R}}$  exceeds  $T_{\text{D}}$ , this is not justified since there has been an early period in which axions were in thermal equilibrium. In this period, their production and annihilation proceeded at equal rates. Thereafter, they decoupled as hot thermal relics at  $T_{\text{D}}$ , where all Standard Model particles are effectively massless. The present yield of those thermal relic axions is then given by  $Y_a^{\text{eq}} = n_a^{\text{eq}}/s \approx 2.6 \times 10^{-3}$ . In Fig. 3 this value is indicated by the horizontal lines. In fact, the thermally produced yield cannot exceed  $Y_a^{\text{eq}}$ . In scenarios with  $T_{\text{R}}$  such that (13) turns out to be close to or greater than  $Y_a^{\text{eq}}$ , disappearance processes have to be taken into account. The resulting axion yield from thermal processes will then respect  $Y_a^{\text{eq}}$  as the upper limit. For example, for  $f_{\text{PQ}} = 10^9$  GeV, this yield would show a dependence on the reheating temperature  $T_{\text{R}}$  that is very similar to the one shown by the dotted line in Fig. 3. The only difference will be a smooth transition instead of the kink at  $Y_a^{\text{TP}} = Y_a^{\text{eq}}$ .

*Axion decoupling temperature*—The kinks in Fig. 3 indicate the critical  $T_{\text{R}}$  value which separates scenarios with thermal relic axions from those in which axions have never been in thermal equilibrium. Thus, for a given  $f_{\text{PQ}}$ ,

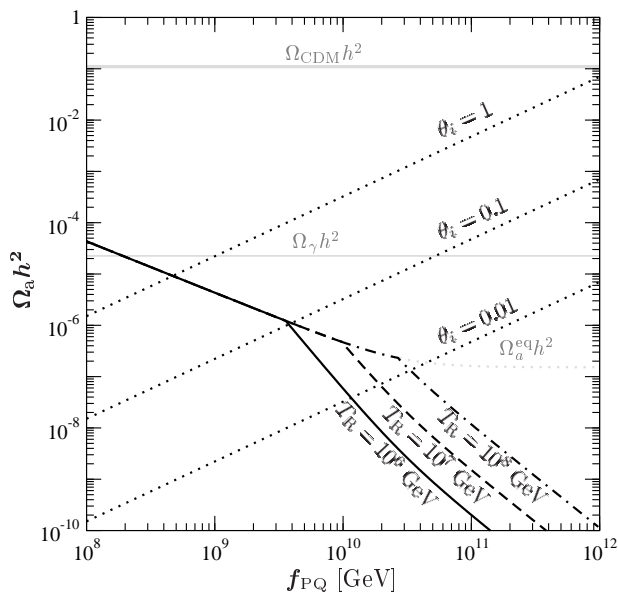


FIG. 4. The axion density parameter from thermal processes for  $T_R = 10^6$  GeV (solid),  $10^7$  GeV (dashed) and  $10^8$  GeV (dash-dotted) and the one from the misalignment mechanism for  $\theta_i = 1, 0.1,$  and  $0.01$  (dotted). The density parameters for thermal relic axions, photons, and cold dark matter are indicated respectively by the gray dotted line ( $\Omega_a^{\text{eq}} h^2$ ), the gray thin line ( $\Omega_\gamma h^2$ ), and the gray horizontal bar ( $\Omega_{\text{CDM}} h^2$ ).

this critical  $T_R$  value allows us to extract an estimate of the axion decoupling temperature  $T_D$ . We find that our numerical results are well described by

$$T_D \approx 9.6 \times 10^7 \text{ GeV} \left( \frac{f_{\text{PQ}}}{10^{10} \text{ GeV}} \right)^{2.246}. \quad (15)$$

In a previous study [3], the decoupling of axions that were in thermal equilibrium in the QGP was calculated. When following [3] but including (14), we find that the temperature at which the axion yield from thermal processes started to differ by more than 5% from  $Y_a^{\text{eq}}$  agrees basically with (15). The axion interaction rate  $\Gamma$  equals  $H$  already at temperatures about a factor four below (15) which however amounts to a different definition of  $T_D$ .

*Axion density parameter*—Since also thermally produced axions have basically a thermal spectrum, we find that the density parameter from thermal processes in the primordial plasma can be described approximately by

$$\Omega_a^{\text{TP/eq}} h^2 \simeq \sqrt{\langle p_{a,0} \rangle^2 + m_a^2} Y_a^{\text{TP/eq}} s(T_0) h^2 / \rho_c \quad (16)$$

with present average momentum  $\langle p_{a,0} \rangle = 2.701 T_{a,0}$  given by the present axion temperature  $T_{a,0} = 0.332 T_0 \simeq 0.08$  meV, where  $T_0 \simeq 0.235$  meV is the present cosmic microwave background temperature,  $h \simeq 0.7$  is Hubble's constant in units of 100 km/Mpc/s and  $\rho_c / [s(T_0) h^2] = 3.6 \times 10^{-9}$  GeV. A comparison of  $T_{a,0}$  with the axion mass

$m_a \simeq 0.6 \text{ meV} (10^{10} \text{ GeV} / f_{\text{PQ}})$  shows that this axion population is still relativistic today for  $f_{\text{PQ}} \gtrsim 10^{11}$  GeV.

In Fig. 4 the solid, dashed, and dash-dotted lines show  $\Omega_a^{\text{TP/eq}} h^2$  for  $T_R = 10^6, 10^7,$  and  $10^8$  GeV, respectively. In the  $f_{\text{PQ}}$  region to the right (left) of the respective kink, in which  $T_R < T_D$  ( $T_R > T_D$ ) holds,  $\Omega_a^{\text{TP/eq}} h^2$  applies which behaves as  $\propto f_{\text{PQ}}^{-3} (f_{\text{PQ}}^{-1})$  for  $m_a \gg T_{a,0}$  and as  $\propto f_{\text{PQ}}^{-2} (f_{\text{PQ}}^0)$  for  $m_a \ll T_{a,0}$ . The gray dotted curve shows  $\Omega_a^{\text{eq}} h^2$  for higher  $T_R$  with  $T_R > T_D$  and also indicates an upper limit on the thermally produced axion density. Even  $\Omega_a^{\text{eq}} h^2$  stays well below the cold dark matter density  $\Omega_{\text{CDM}} h^2 \simeq 0.1$  (gray horizontal bar) and also below the photon density  $\Omega_\gamma h^2 \simeq 2.5 \times 10^{-5}$  (gray thin line) [5] in the allowed  $f_{\text{PQ}}$  range (2). There, also the current hot dark matter limits are safely respected [12].

In cosmological settings with  $T_R > T_D$ , also axions produced non-thermally before axion decoupling (e.g., in inflaton decays) will be thermalized resulting in  $\Omega_a^{\text{eq}} h^2$ . The axion condensate from the misalignment mechanism however is not affected—independent of the hierarchy between  $T_R$  and  $T_R$ —since thermal axion production in the QGP is negligible at  $T \lesssim 1$  GeV. Thus, the associated density  $\Omega_a^{\text{MIS}} h^2 \sim 0.07 \theta_i^2 (f_{\text{PQ}} / 10^{12} \text{ GeV})^{7/6}$  [1, 2] can coexist with  $\Omega_a^{\text{TP/eq}} h^2$  and is governed by the misalignment angle  $\theta_i$  as illustrated by the dotted lines in Fig. 4. Thereby, the combination of the axion cold dark matter condensate with the axions from thermal processes,  $\Omega_a h^2 = \Omega_a^{\text{MIS}} h^2 + \Omega_a^{\text{TP/eq}} h^2$ , give the analog of a Lee–Weinberg curve. Taking into account the relation between  $f_{\text{PQ}}$  and  $m_a$ , this is exactly the type of curve that can be inferred from Fig. 4. Here our calculation of thermal axion production in the QGP allows us to cover for the first time also cosmological settings with  $T_R < T_D$ .

We are grateful to Thomas Hahn, Josef Pradler, Georg Raffelt, and Javier Redondo for valuable discussions. This research was partially supported by the Cluster of Excellence ‘Origin and Structure of the Universe.’

- 
- [1] P. Sikivie, Lect. Notes Phys. **741**, 19 (2008)
  - [2] J.E. Kim, G. Carosi (2008), 0807.3125
  - [3] E. Masso, F. Rota, G. Zsembinski, Phys. Rev. **D66**, 023004 (2002)
  - [4] G.G. Raffelt, Lect. Notes Phys. **741**, 51 (2008)
  - [5] C. Amsler et al. (Particle Data Group), Phys. Lett. **B667**, 1 (2008)
  - [6] S. Chang, K. Choi, Phys. Lett. **B316**, 51 (1993)
  - [7] S. Hannestad, A. Mirizzi, G. Raffelt, JCAP **0507**, 002 (2005)
  - [8] M.S. Turner, Phys. Rev. Lett. **59**, 2489 (1987)
  - [9] E. Braaten, R.D. Pisarski, Nucl. Phys. **B337**, 569 (1990)
  - [10] E. Braaten, T.C. Yuan, Phys. Rev. Lett. **66**, 2183 (1991)
  - [11] M. Bolz, A. Brandenburg, W. Buchmüller, Nucl. Phys. **B606**, 518 (2001); *ibid.* **B790** 336 (2008)
  - [12] S. Hannestad, A. Mirizzi, G.G. Raffelt, Y.Y.Y. Wong, JCAP **1008**, 001 (2010)